Quantitative spectromicroscopy from inelastically scattered photoelectrons in the hard X-ray range

Renault, O; Zborowski, Charlotte; Risterucci, P; Wiemann, C; Grenet, G; Schneider, C M; Tougaard, Sven Mosbæk

Published in:
Applied Physics Letters

DOI:
10.1063/1.4955427

Publication date:
2016

Document version
Publisher's PDF, also known as Version of record

Quantitative spectromicroscopy from inelastically scattered photoelectrons in the hard X-ray range

O. Renault,[1,a)] C. Zborowski,[1] P. Risterucci,[1] C. Wiemann,[2] G. Grenet,[3] C. M. Schneider,[2] and S. Tougaard[4]
[1]*Univ. Grenoble Alpes, F-38000 Grenoble, France and CEA, LETI, MINATEC Campus, F-38054 Grenoble, France*
[2]*Peter Grünberg Institute (PGI-6) and JARA-FIT, Research Center Jülich, D-52425 Jülich, Germany*
[3]*Institut des Nanotechnologies de Lyon, Ecole Centrale, 69134 Ecully Cedex, France*
[4]*Department of Physics, Chemistry and Pharmacy, University of Southern Denmark, DK-5230 Odense M, Denmark*

(Received 10 March 2016; accepted 24 June 2016; published online 5 July 2016)

We demonstrate quantitative, highly bulk-sensitive x-ray photoelectron emission microscopy by analysis of inelastically scattered photoelectrons in the hard X-ray range, enabling elemental depth distribution analysis in deeply buried layers. We show results on patterned structures used in electrical testing of high electron mobility power transistor devices with an epitaxial $Al_{0.25}Ga_{0.75}N$ channel and a Ti/Al metal contact. From the image series taken over an energy range of up to 120 eV in the Ti 1*s* loss feature region and over a typical 100 μm field of view, one can accurately retrieve, using background analysis together with an optimized scattering cross-section, the Ti depth distribution from 14 nm up to 25 nm below the surface. The method paves the way to multi-elemental, bulk-sensitive 3D imaging and investigation of phenomena at deeply buried interfaces and microscopic scales by photoemission. *Published by AIP Publishing.*
[http://dx.doi.org/10.1063/1.4955427]

The advent of Hard X-ray Photoelectron Spectroscopy (HAXPES) exploiting third generation synchrotron radiation sources has enabled a step forward in photoemission for accessing information from buried interfaces.[1–3] Recently, HAXPES was further extended to the microscopic scale with Hard X-ray Photoelectron Emission Microscopy (HAXPEEM), and the possibility to retrieve microscopic, bulk sensitive information from core-level spectromicroscopy.[4] This technique is to date the only way to perform laterally resolved HAXPES, as small-spot methods derived from Scanning Photoemission Microscopy (SPEM) have still not been applied to the hard x-ray range. HAXPEEM further expands on previous PEEM-based, highly depth-resolved methods employing soft X-ray standing waves,[5,6] but is unfortunately restricted to a limited depth range of some nm. Particularly, it enables the analysis of buried interfaces in well-defined patterned structures as frequently encountered in device technology, where the active layer of a functional material is part of a more or less complex stacked structure with a top electrode.[4–6] Resistive memory devices are an important example in this field, where in some cases the switching mechanism from a high resistive to a low resistive state deals with an accumulation of oxygen vacancies at the oxide/electrode interface.[7,8] This particular case illustrates the importance of spatial resolution in HAXPES, which becomes also mandatory when physical characterization and electrical testing have to be performed on the same test device structure. However, in most practical cases, the thickness of the electrode overlayer is larger than the maximal probing depth accessible with core-level photoelectrons, which is about three times the inelastic mean-free path (IMFP). With excitation energies of 3–8 keV, the probing depth is typically smaller than 20 nm, making it necessary to study model devices with a thinner electrode, which may no longer be representative of the real conditions. Moreover, quantification with core-level spectra alone from deeply buried elements can lead to large errors, especially in the case of complex distribution profiles.[9] One way to overcome this limitation is to exploit inelastically scattered photoelectrons[10,11] providing information from deeply buried interfaces up to 50 nm, as was recently shown in HAXPES.[12] Indeed, these latter electrons originate from typical depths as high as 8 times the IMFP[10] and constitute the so-called inelastic background to lower kinetic energy of the core-level photoemission spectrum. This background contains specific information regarding the depth distribution of the corresponding element which can be retrieved in a quantitative way, following Tougaard's theoretical and practical framework originally developed for XPS.[10,11,13] Applied to HAXPES, the method has, similarly to XPS, the potential to determine and quantify complex depth distributions of several elements such as diffusion profiles, but still lacks microscopic capabilities.

In this letter, we present an HAXPEEM method where the spectromicroscopic information arises from inelastically scattered photoelectrons and is treated in a quantitative way by inelastic background analysis for probing deeply buried interfaces previously not accessible at microscopic scales by photoemission. Unlike microprobe XPS providing a spectrum from areas of interest as small as ~10 μm with laboratory X-ray sources and less than 100 nm with synchrotron radiation X-rays, the key advantage of XPEEM is the full-field, spectroscopic imaging capability, enabling one to ultimately retrieve one spectrum at each image pixel. Here, we

a)E-mail: olivier.renault@cea.fr

focus on the quantitative analysis of energy-loss spectra from different areas within the HAXPEEM microscope field of view (FoV), as a necessary step for further developments regarding the mapping from analysis of spectra-at-pixels. An example is taken with a power transistor device structure based on a 2D electron gas in AlGaN with a top ohmic Ti/Al contact, the formation of which is crucial to understand for further optimizing device operation.

The study is performed on a technologically relevant stack of GaN-based High Electron Mobility Transistor (HEMT). This sample presents two metal overlayers of aluminum (15 nm) and titanium (10 nm) deposited by Electron Beam Physical Vapor Deposition (EBPVD) on a $Al_{0.25}Ga_{0.75}N$ (11 nm)/AlN (1 nm)/GaN (some μm) heterostructure epitaxially grown by Metal-Organic Chemical Vapor Deposition (MOCVD) on a Si(111) substrate. Subsequently, so-called TLM (Transfer Length Method) structures used for resistivity measurements were patterned by UV lithography and the lift-off process. The resulting sample was analyzed prior to any activation annealing or sputtering so we rely on the nominal layer thicknesses shown in Fig. 1. The nominal thicknesses were further confirmed by Energy-Dispersive X-ray spectrometry (EDX) performed in a High Resolution Transmission Electron Microscope on a cross section prepared by focus ion beam milling in a TLM contact identical to that observed in HAXPEEM.

HAXPEEM was performed with a NanoESCA MkII spectromicroscope (ScientaOmicron) from Forschungzentrum Jülich[4] as a temporarily installed endstation at the P09 beamline of PETRA III (Deutsches Elektronen-Synchrotron DESY, Hamburg).[14] The photon energy was set to 8 keV. The image chain at the exit of the imaging spectrometer (aberration-compensated double hemispherical analyzer) consists of a double multichannel plate (MCP), a phosphor screen, and a CCD camera. Image series were recorded over the extended Ti 1s region, namely, including the core-level peak and its energy-loss tail up to 120 eV to the lower kinetic energy side. More precisely, the imaging unit was operated in the analogue mode, with the MCP acting as a linear amplifier and the CCD acquiring long exposure (30 s per image). The kinetic energy range was scanned from 2909 to 3099 eV. The energy step was 0.5 eV and the field of view (FoV) 97 μm. The pass energy of the imaging spectrometer was set to 200 eV and its entrance slit to 1 mm, yielding an overall energy resolution (photon band width included) of 2 eV. The contrast aperture was set to 500 μm, providing a theoretical lateral resolution of 500 nm. The image series obtained provide ultimately one core-level and energy loss spectrum per pixel. However, for a better local statistics on the energy loss spectra, these latter were generated from larger regions, on the Ti/Al contact.

Figure 2 presents the Ti 1s energy-loss spectra generated over several regions on the Ti/Al contact highlighted as a bright stripe on both HAXPEEM images presented. All spectra display identical shapes, indicative qualitatively of a uniform Ti depth distribution over the stripe. We note that some Ti 1s intensity is also detected on the dark stripe where the bare AlGaN substrate is solely expected. This artifact is due to scattering in the light optical system, between the screen and the CCD camera.[4] The image taken using inelastically scattered photoelectrons in the far energy loss region ($E\text{-}E_F = 2931$ eV), 107 eV kinetic energy from the core-level peak, displays an increased intensity compared to the core-level image taken at the peak energy ($E\text{-}E_F = 3038$ eV). This image is therefore more useful to study the buried Ti layer and may also provide an enhanced effective lateral resolution through the increased counting statistics. Also, it can be quite clearly seen that the energy-loss image highlights, on the right hand side, the edge of the stripe (white arrow), which is not so obvious from the core-level image. This points to the fact that substantial information can be obtained from the energy-loss image of a buried element, particularly if the core-level peak is weak due to either a small amount of substance[12] and/or a weak photoionization cross-section. Looking closer at the Ti 1s micro-spectra on the bright stripe, we see that the first plasmon loss peak has higher intensity than the Ti 1s core level peak at 3038 eV kinetic energy, in agreement with the buried character of Ti in the region of interest. The separation between these two peaks is 15.6 eV, which is in good agreement with the plasmon excitation energy in pure Al (15.8 eV).[15]

Next, we concentrate on the quantitative, so-called inelastic background analysis[10] of the energy-loss Ti 1s micro-spectra of Fig. 2. We have not considered the analysis of the spectra from the dark stripe, first because of the artifact on the Ti 1s emission; another reason is that regarding Al 1s, the depth distribution of Al in distinct layers makes the analysis more difficult. The principle of the quantitative analysis consists in subtracting from the photoelectron spectrum $J(E,\Omega)$ measured within the solid angle Ω, the extrinsic contributions to the energy losses, which depend upon the depth distribution $f(z)$ of the considered element. One obtains a corrected or original spectrum, $F(E_0,\Omega)$, only accounting for intrinsic contributions, including shake-up excitations, of

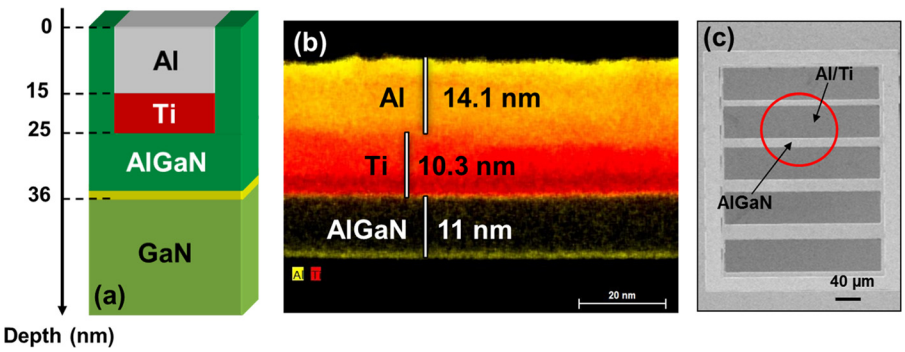

FIG. 1. (a) Nominal elemental depth distribution of the multilayer HEMT structure considered for imaging. (b) Measured depth distribution by TEM-EDX on a cross-section taken in between the patterns shown on the optical microscopy image (c). The red circle represents the HAXPEEM field of view.

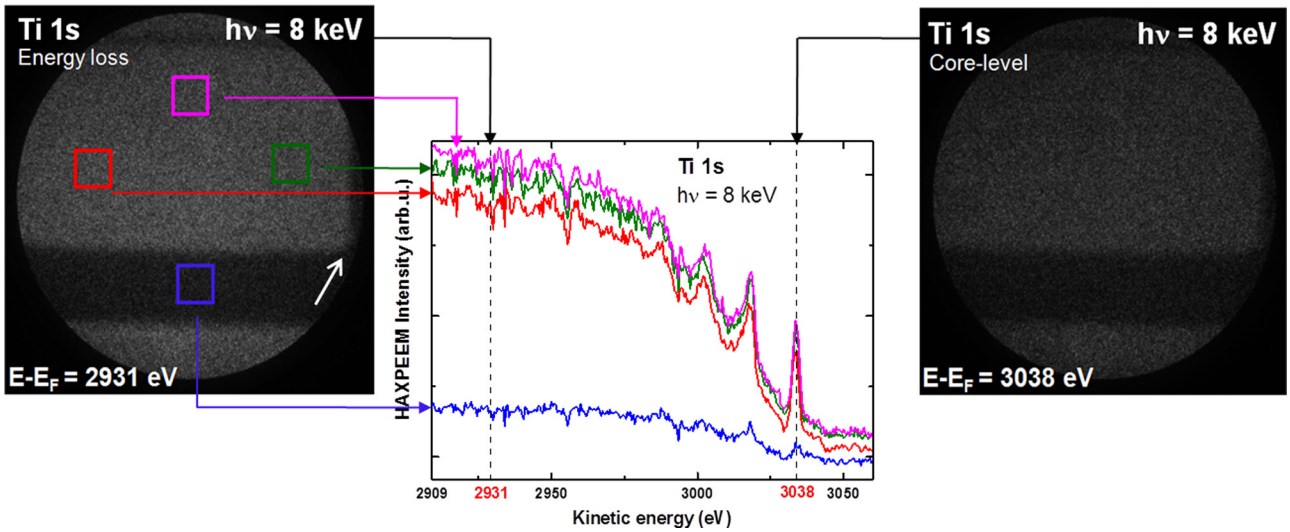

FIG. 2. HAXPEEM micro-spectra of the extended Ti 1s photoelectron energy-loss region and corresponding images at the core-level peak (3038 eV, right) and in the far inelastic energy loss region (2931 eV, left). The image field of view is 97 μm, and the size of the area of interest, 10×10 μm. Both images are displayed within the same grayscale dynamic. The arrow on the energy-loss image points to the edge of the stripe.

primary photoelectrons. This formalism relies on a two-step photoemission model,[10,11] assuming that the intrinsic and extrinsic effects are decoupled. The surface excitations are neglected in this model and replaced by a bulk excitation cross-section: this approximation is particularly suitable in HAXPES where surface excitations are less prominent. Then, we can express the measured spectrum as[10,11]

$$J(E,\Omega) = \frac{1}{2\pi}\int F(E_0,\Omega)dE_0 \int\int f(z)e^{is(E_0-E)}e^{\frac{-z}{\cos\theta}\sum(s)}dsdz, \tag{1}$$

with

$$\sum(s) = \frac{1}{\lambda(E)} - \int_0^\infty K(T)e^{-isT}dT, \tag{2}$$

where E_0 is the initial energy of the photoelectron and E the final energy after having travelled the distance $\frac{z}{\cos\theta}$. $K(E,T) \approx K(T)$ is the inelastic-scattering cross section which represents the probability of an electron to lose the energy $T = E_0 - E$ and λ is the inelastic mean free path which depends on E. In Eq. (1), $J(E,\Omega)$ is the measured spectrum, while we want to determine $F(E_0,\Omega)$. To this end, it was shown[16] that the integral equation (Eq. (1)) can be solved numerically for $F(E_0,\Omega)$ by discrete fast Fourier transformation and the user friendly QUASES-Tougaard software[13] was developed to perform these calculations.

Figure 3 presents the background modelling of the Ti 1s HAXPEEM spectrum displayed in Fig. 2. The only input in the software is $\lambda(E)$ and $K(T)$ while the depth distribution $f(z)$ is varied until a good match is obtained over typically ~30–120 eV to lower kinetic energy below the Ti 1s peak,[10,11,13] between the calculated and the measured spectrum. The effective λ is taken as a weighted average of individual λ calculated using the TPP-2M formula[17–19] for each of the layers located above, according to their nominal thicknesses. The resulting, effective λ value for Ti 1s photoelectrons is determined as 5.5 nm. Therefore, the corresponding probing depth ($\sim 8\lambda$) with inelastically scattered photoelectrons in the energy-loss region of interest here is up to 44 nm, and consequently, the entire 10 nm-thick Ti layer below the 15 nm-thick Al surface layer can be probed. For the choice of the scattering cross-section, we first note that the cross-section of pure Al presents a marked plasmon peak, of which both single and double excitations are clearly visible in the 35 eV energy loss region below the Ti 1s peak (Fig. 2). A universal, broad and featureless cross-section[20] is therefore not suitable in the case of sharp plasmon structures.[12] However, we found that the use of a weighted average of individual K(T) functions of pure Ti, pure Al, and universal cross-sections provides a better match (and therefore a more accurate determination of the depth distribution) than just using a single Al cross-section. This is in agreement, as explained above, with the large probing depth which includes the entire Ti buried layer, meaning that the Ti 1s photoelectron is transported across layers of Ti and Al. The blend with the two-parameter universal cross-section[20] is believed to originate from the surface Al oxide layer and maybe also be associated with particular microstructures of the deposited Ti and Al films. The cross-sections for Al[21] and Ti were determined from reflection electron energy-loss spectroscopy using the QUASES-XS-REELS software.[22] The optimal blend of individual Ti, Al, and universal cross-sections is $K_{eff}(T) = 0.28 \times K_{Univ}(T) + 0.27 \times K_{Ti}(T) + 0.45 \times K_{Al}(T)$. In

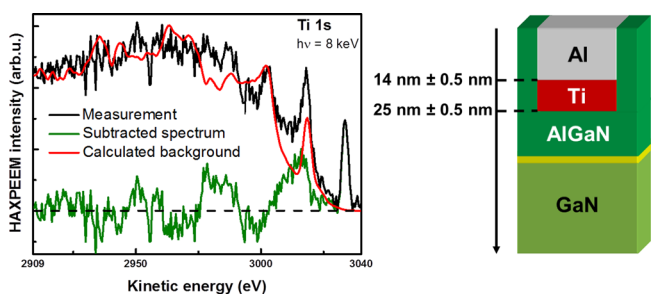

FIG. 3. Inelastic background analysis of the Ti 1s HAXPEEM energy-loss micro-spectrum from the pink region of Fig. 2.

other similar cases, we recently found that using such blends of cross-sections is necessary to improve the reliability of the inelastic background analysis in HAXPES of deeply buried layers.[23] Here, using this blend, the inelastic background is best reproduced, over the 25–120 eV energy loss range, for a Ti depth distribution ranging between 14 ± 0.5 nm and $25\,\text{nm} \pm 1$ nm below the surface. These figures are in very good agreement with the overlayer structure determined by TEM-EDX (Fig. 1). The question arises now to which extent the modelled background is sensitive to variations, at the nm-scale, of the effective Ti depth distribution. This is because the background spectrum is quite noisy due to the microscopic character of the emitting area; we found, however, that considering a larger area by averaging over the entire Ti/Al stripe did not significantly change the result. In a previous study,[12] we faced a similar issue for a different reason, namely, a small buried elemental concentration: we showed that the derived, correct depth distribution corresponded to a minimum in the X^2 residual of the modelling. Similarly here, we have performed several alternative modeling using different depths of both the top and the bottom Ti interface (varied by a typical ± 0.5 nm increment) and could confirm that the error (namely, the normalized integrated area of the corrected spectrum), for the 14 to 25 nm depth distribution corresponds to a minimum. The use of a smaller increment did not result in significant changes in the modeling; from this observation, we determine the uncertainty of ± 0.5 nm in the depth derived for each interface. As seen in Fig. 4, significantly increased errors are observed for deviations larger than $\pm 10\%$ from the optimal 14 nm and 25 nm interface depths. Extending the described method to the analysis of spectra-at-pixels to allow depth-resolved mapping of the Ti 1s elemental distribution is of high interest towards 3D-imaging in HAXPES. Such a development is actually ongoing in our group, and is based on previous work performed in XPS imaging.[24,25] The challenge in HAXPES 3D-imaging is to combine a suitable automated procedure for background analysis, as the one described here, with noise reduction and multivariate methods such as Principal Component Analysis suitable for treating very low-intensity spectra. Last, but not least, it is useful to summarize the pros and cons of the technique developed here. As mentioned before, the method is able to determine precisely elemental depth distributions over several tens of nm in a non-destructive way and ultimately at the nm scale, with, as reported previously,[11] similar accuracy in the case of complex distribution profiles; the microscopic capability cannot be reached by laboratory techniques such as X-ray reflectivity or spectroscopic ellipsometry. It is restricted to elemental distributions, but chemical information can be derived by complementary core-level analysis over smaller depth, cross-checked by analyzing overlapping depth distributions of different elements.

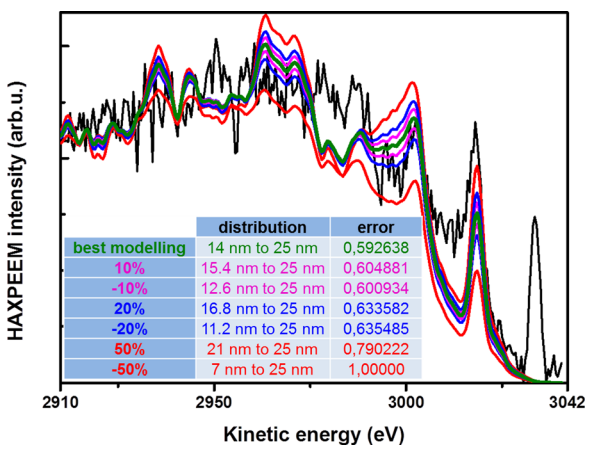

FIG. 4. Calculation of the best modeling for the inelastic background analysis comparing different depth distributions using the same cross-section.

In conclusion, we have shown that spectroscopic imaging with HAXPEEM using inelastically scattered photoelectrons excited with hard x-rays enhances the sensitivity to deeply buried layers. We have performed a quantitative inelastic background analysis within Tougaard's framework to retrieve at the microscopic scale, in a reliable way, the elemental depth distribution over 14–25 nm depth below the surface. The method paves the way to the investigation of phenomena at deeply buried interfaces at the microscopic scale by photoemission.

We thank A. Torrès (CEA-LETI) for providing the patterned sample. Part of this work was performed at the Nanocharacterization Platform of CEA-MINATEC. DESY is acknowledged for providing beamtime and the P09 beamline staff for assistance during the experiment.

[1]K. Kobayashi, Nucl. Instrum. Methods Phys. Res., Sect. A **601**(1–2), 32 (2009).
[2]W. Drube, J. Electron Spectrosc. Relat. Phenom. **190**, 125 (2013).
[3]K. Siegbahn, Nucl. Instrum. Methods Phys. Res., Sect. A **547**(1), 1 (2005).
[4]M. Patt, C. Wiemann, N. Weber, M. Escher, A. Gloskovskii, W. Drube, M. Merkel, and C. M. Schneider, Rev. Sci. Instrum. **85**(11), 113704 (2014).
[5]F. Kronast, R. Ovsyannikov, A. Kaiser, C. Wiemann, S. H. Yang, D. E. Bürgler, R. Schreiber, F. Salmassi, P. Fischer, H. A. Durr, C. M. Schneider, W. Eberhardt, and C. S. Fadley, Appl. Phys. Lett. **93**(24), 243116 (2008).
[6]A. X. Gray, F. Kronast, C. Papp, S. H. Yang, S. Cramm, I. P. Krug, F. Salmassi, E. M. Gullikson, D. L. Hilken, E. H. Anderson, P. Fischer, H. A. Dürr, C. M. Schneider, and C. S. Fadley, Appl. Phys. Lett. **97**(6), 062503 (2010).
[7]C. Lenser, M. Patt, S. Menzel, A. Köhl, C. Wiemann, C. M. Schneider, R. Waser, and R. Dittmann, Adv. Funct. Mater. **24**(28), 4466 (2014).
[8]M. Sowinska, T. Bertaud, D. Walczyk, S. Thiess, P. Calka, L. Alff, C. Walczyk, and T. Schroeder, J. Appl. Phys. **115**(20), 204509 (2014).
[9]It is only possible to use core-peak data for atoms at $>3 \times$ IMFP if, and only if it is certain that there are absolutely no atom at depths $<3 \times$ IMFP. The contribution from just a few % concentration at, say $0.5 \times$ IMFP depth would completely overshadow the contribution from atoms located deeper at ~3–5 IMFP.
[10]S. Tougaard, Surf. Interface Anal. **26**(4), 249 (1998).
[11]S. Tougaard, J. Electron Spectrosc. Relat. Phenom. **178–179**, 128 (2010).
[12]P. Risterucci, O. Renault, E. Martinez, B. Detlefs, V. Delaye, J. Zegenhagen, C. Gaumer, G. Grenet, and S. Tougaard, Appl. Phys. Lett. **104**(5), 051608 (2014).
[13]See http://www.quases.com/ for S. Tougaard, Software Packages to Characterize Surface nano-Structures by Analysis of Electron Spectra (2015).
[14]J. Strempfer, S. Francoual, D. Reuther, D. K. Shukla, A. Skaugen, H. Schulte-Schrepping, T. Kracht, and H. Franz, J. Synchrotron Radiat. **20**, 541 (2013).
[15]P. Braun, M. Arias, H. Stori, and F. P. Viehbock, Surf. Sci. **126**, 714 (1983).
[16]S. Tougaard and H. S. Hansen, Surf. Interface Anal. **14**(11), 730 (1989).

[17]S. Tanuma, C. J. Powell, and D. R. Penn, Surf. Interface Anal. **20**(1), 77 (1993).
[18]S. Tanuma, C. J. Powell, and D. R. Penn, Surf. Interface Anal. **43**(3), 689 (2011).
[19]H. Shinotsuka, S. Tanuma, C. J. Powell, and D. R. Penn, Surf. Interface Anal. **47**(9), 871 (2015).
[20]S. Tougaard, Surf. Interface Anal. **25**, 137 (1997).
[21]S. Tougaard and J. Kraaer, Phys. Rev. B **43**(2), 1651 (1991).
[22]S. Tougaard and I. Chorkendorff, Phys. Rev. B **35**(13), 6570 (1987).
[23]P. Risterucci, S. Tougaard, C. Zborowski, and O. Renault (unpublished).
[24]S. Hajati, S. Coultas, C. Blomfield, and S. Tougaard, Surf. Interface Anal. **40**(3–4), 688 (2008).
[25]S. Hajati, S. Coultas, C. Blomfield, and S. Tougaard, Surf. Sci. **600**(15), 3015 (2006).